PZT THIN FILMS FOR MICRO SENSORS AND ACTUATORS

P. Muralt
Laboratoire de Céramique,
Ecole Polytechnique Fédérale de Lausanne (EPFL),
Lausanne, Switzerland

INVITED PAPER
24th International Conference on Microelectronics, MIEL'96
32nd Symposium on Devices and Materials, SD'96
September 25.-September 27., 1996, Nova Gorica, Slovenia

Key word: micromechanical systems, PZT thin films, integration onto silicon substrates, ultrasonic micromotors, IR detectors, PZT ferroelectric materials, MOCVD, Metal-Organic-Chemical Vapor Deposition, MOD, Metal-Organic Decomposition, piezoelectric microactuators

Abstract: The paper reviews different aspects of deposition, integration, and device fabrication of $PbZr_xTi_{1-x}O_3$ (PZT) films for application in micromechanical systems. The deposition of such films and the principal processes for their integration onto silicon substrates are now fairly well mastered. Current efforts concentrate on tailoring the film properties for the various applications, and on optimization of the device designs and patterning processes. Current work on an ultrasonic micromotor and a pyroelectric IR detector is presented and discussed.

PZT tanke plasti za mikro senzorje in aktivatorje

Ključne besede: sistemi elektromehanski, PZT plasti tanke, integracija na substrate silicijeve, mikromotorji ultrazvočni, IR detektorji sevanja infrardečega, PZT materiali feroelektrični, MOCVD nanosi kemični s paro kovina-snov organska, MOD dekompozicija kovinsko-organska, mikroaktivatorji piezoelektrični

Povzetek: Prispevek v pregledni obliki podaja različne aspekte nanosa, integracije in izdelave komponent s $PbZr_xTi_{1-x}O_3$ (PZT) filmi za uporabo v mikromehanskih sistemih. Nanos teh filmov, kakor tudi načini njihove integracije na silicijeve substrate so danes že precej poznani in dozoreli. Trenutno so napori usmerjeni v prilagajanje lastnosti plasti različnim uporabam, optimizaciji načrtovanja komponent, ki jih uporabljajo, kakor tudi procesom fotolitografije. V prispevku prikazujemo trenutno stanje in delo na področju uporabe teh plasti pri izvedbi ultrazvočnega motorja in piroelektričnega IR detektorja.

1. INTRODUCTION

In general, thin films allow an increase in functionality of devices by miniaturization, and reduction of fabrication costs by batch processing. Integration onto silicon offers the possibility to apply silicon micromachining techniques, and to integrate sensor and electronics on the same substrate. In recent years, a number of research groups have concentrated their efforts on the preparation of the ferroelectric material $PbZr_xTi_{1-x}O_3$ (PZT) as a thin film, and its integration onto silicon substrates for the development of ferroelectric memories, piezoelectric actuators and sensors, and pyroelectric infra-red detectors. Various obstacles were and are encountered on the way to achieving a perfect film for a given device. High quality films require deposition or annealing temperatures of around 600 °C in oxygen or air. For this reason the deposition process often is not compatible with other materials in the device: Interdiffusion and/or delamination may occur. Film growth conditions and integration technology influence each other and both affect the device performance. In this paper different aspects of deposition, integration, device fabrication and applications of PZT films are reviewed.

2. THIN FILM DEPOSITION

A historical review of ferroelectric thin film deposition is given in ref. /1/. Whereas before 1990 mostly physical deposition techniques (evaporation, RF sputtering) were applied, chemical methods dominate at present. Metal-organic-chemical vapor deposition (MOCVD) is the preferred technique for IC applications, because of its superior step coverage. Metal-organic decomposition (MOD), with or without sol-gel reactions, is likely to emerge as the leading method for actuator and sensor applications because of the low investment needed. Sputtering will keep its place in cases where a lowering of the deposition temperature is of importance.

High quality PZT thin films can be grown with in-situ deposition techniques like sputtering at 500 to 550 °C /2,3/, or with MOCVD at 700 °C /4,5/. The post-anneal for sol-gel deposition has to be carried out at temperatures between 600 and 650°C /6/. All processes usually work with an excess of lead. Lead or PbO desorb quickly from the surface at these temperatures, as long as they are not incorporated in the perovskite lattice. With in-situ deposition techniques one observes a self stabilization

of the lead content at stoichiometry above a critical temperature, even for large quantities of excess lead flux. The critical temperature depends on the deposition method and is 700 °C for $PbTiO_3$ grown by MOCVD /7/, and was found to be lower for sputter deposition (550°C) due to plasma effects /8/.

3. INTEGRATION

The choice of substrate is usually dictated by the application or by the need to lower production costs. Hence, the substrate is often not the most ideal one for growing the ferroelectric thin film. The integration technology has to solve adhesion and interdiffusion problems and should provide a mean to arrive at the required film microstructure. Finally, the patterning, i.e. the selective etching of the involved films, has to be mastered.

The most important substrate for micro systems is silicon. High quality PZT films cannot be grown directly on it. Buffer layers are needed to prevent interdiffusion and oxidation reactions. For most applications, the PZT film has to be grown on an electrode, which obviously should neither oxidize nor become insulating. The most often reported materials include platinum, and the metal oxides RuO_2 (rutile structure) /9/ and (La,Sr)CoO_3 (LSC, perovskite structure) /10/. Usually, the chemical barrier function is provided by two or more layers, including the electrode. PZT/Pt/Ti/SiO_2/Si is the most widely applied sequence, where the Ti is needed as an adhesion layer. Platinum does not inhibit the diffusion of Ti to the PZT side, where it reacts with oxygen and serves as nucleation centers for PZT. There is also evidence that oxygen migrates along the grain boundaries through the platinum film and reacts with the Ti layer /11/. For stable electrodes the latter has to be preoxidized /11/. Barrier schemes with insulating films, such as SiO_2 and Si_3N_4, cannot be applied when a direct electrical contact to a silicon or metal substrate is required. In this case, RuO_2 electrodes are superior to platinum electrodes. In combination with a second metal (e.g. Cr), which stops the residual oxygen diffusion, RuO_2 allows the growth of PZT on very reactive refractory metals, such as zirconium (see fig. 1) /12/.

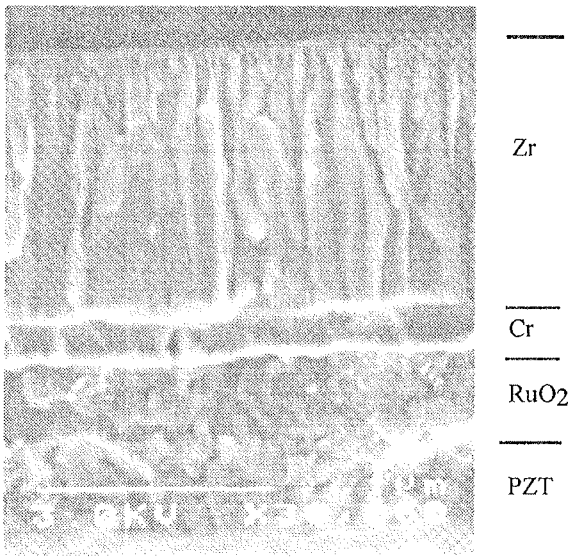

Fig. 1: Scanning electron microscopy image of a cross section of the layer stack PZT/RuO_2/Cr/Zr (the photo is up-side-down) deposited for piezoelectric activation of thin zirconium membranes (from ref. /12/, 0.6μm sputtered PZT).

The requirements with respect to film microstructure depend on the application. For piezoelectric applications polycrystalline films may be sufficient. However, for pyroelectric applications it is advantageous to have a textured film with the ferroelectric polarization perpendicular to the substrate plane. This is not easy to obtain for $PbTiO_3$, in which an additional complication arises due to the cubic-to-tetragonal ferroelectric phase transition below the deposition temperature. With a perfectly textured (100) film in the cubic high temperature phase, only 1/3 of perpendicular polarization is obtained a priori below the phase transition. The degree of perpendicular polarization (c-axis orientation) finally obtained at room temperature is strongly influenced by the thermal expansion mismatch between substrate and film /13,14/. Well c-axis oriented films are obtained on $SrTiO_3$ /15/ and MgO /16/ substrates, because their high thermal expansion compresses the film upon cooling from the growth temperature and the larger c-axis is switched out of the plane.

Due to its much smaller thermal expansion, this does not happen on silicon substrates. Even worse, if the deposition process yields a tensile stress, as caused by the shrinkage of the sol-gel preparation technique, its stress is compensated by switching the c-axis into the plane and thus useful polarization is lost. Sputter processes allow incorporation of a compressive stress during in-situ deposition, and hence stronger c-axis orientation /3/. With stress measurements as a function of temperature it is in principle possible to determine the degree of c-axis orientation (see fig. 2). Note that stress compensation by 90° domain flipping works only above about 300 °C.

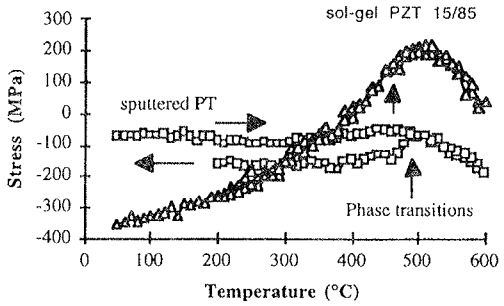

Fig. 2: Film stress vs. temperature curves for a heating/cooling cycle. The curves result from the difference between the substrate curvatures with and without (etched off) P(Z)T film. Positive values indicate tensile stress, while negative indicate compressive stress. The phase transitions are marked as known from bulk ceramics. The intensity ratio I(002)/I(200) of the <100> sputtered film dropped form 1 to 0.8 due to thermal cycling. The sol-gel film exhibited mainly (100) orientation. (The measurements have been performed with a commercial FLX 2900 system).

With sol-gel deposition, (111) oriented PT films turned out to be the better choice. Their pyroelectric coefficient is close to the theoretical value expected for this orientation (60 % of (001) single crystal coefficient), because poling involves only switching of 180° domains.

Textured growth can be controlled by a number of process parameters and by the electrode. The phenomena observed in in-situ sputter deposition do not seem to be so much different from those observed in sol-gel deposition techniques. For the growth of textured PZT films on platinum electrodes /17/ two nucleation regimes are observed:

1. Self orientation of PZT (100). These faces have a lower surface energy and thus the (100) orientation is obtained under certain favorable circumstances. These are: lead excess, which leads to a high mobility; slow nucleation, i.e. no faster nucleation of another orientation takes place; Ti rich at the nucleation interface (The Ti may also come from below the platinum.). With in-situ sputter deposition, (100) nucleation of $PbTiO_3$ works very well, whereas for PZT(100) a $PbTiO_3$(100) template has to be applied (see fig. 3) /8/.

2. Epitaxial orientation of PZT(111) on well textured Pt(111). The close lattice match between these two lattices is not sufficient to assure a good (111) orientation. An additional "glue" is often required. A very effective method consists of applying a 1 to 2 nm thin TiO_2 seed layer. It could be shown /18/ that this film is textured, i.e. it grows epitaxially on Pt(111). This seed layer promotes a quick nucleation of PZT(111), during which it is dissolved in the PZT. The method works as well with in-situ sputter deposition as with sol-gel techniques /18/.

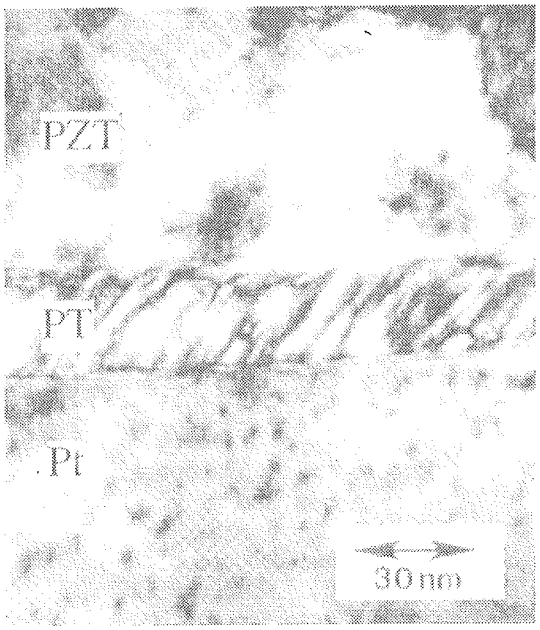

Fig. 3: Transmission electron microscope image of a 30 nm thick $PbTiO_3$ template film between the platinum electrode (bottom) and the PZT film. The oblique stripes are caused by the domain structure of alternating (100) and (001) orientations (from ref. 8).

4. ACTUATORS

Piezoelectricity is a competitive actuation principle for micro-actuators and sensors. Compared to thermal methods (bi-metal and shape memory alloys), piezoelectricity dissipates less heat and can be applied at much higher frequencies. With regard to electrostatic actuation, piezoelectricity demands less complex structures, exhibits a better linearity between applied voltage and force, and yields a larger force output.

4.1 Operation principle

For actuation, the reverse piezoelectric effect is exploited between the E-field (E_3) parallel to the polarization, being perpendicular to the film plane, and the stress perpendicular to the polarization (σ_1 and σ_2) in the film plane. These stresses create a bending moment with respect to the neutral plane of a membrane or cantilever structure. It is clear that the passive part below the piezoelectric film must be at least as thick as the piezoelectric film. Compared to the usual e_{31} coefficient for full clamping, the effective piezoelectric coefficient is enhanced by the fact that the film is free to expand perpendicular to the surface (direction of index 3). For a uniform planar geometry one obtains /19/:

$$\sigma_{1,2} = -e_{31,eff} \cdot E_3 = -\frac{d_{31}}{s_{11}^E + s_{12}^E} \cdot E_3$$

The stress σ_1 can be determined from the resonance frequency shift vs. applied dc field of a membrane containing the piezoelectric film /19/. More often, the strain x_3 perpendicular to the film plane is determined, as it can be accurately measured by means of double side interferometry /20/ without need for structuring the substrate. The so derived coefficient d_{33} is also an effective value, which is lowered by the substrate clamping /21/. In fig. 4 strain and frequency shift (stress) are compared as a function of the applied dc voltage. The two "butterfly" curves look pretty much the same and illustrate how the thickness increase of the film (positive strain) is accompanied by an increasing tensile stress (positive frequency shift) in the film plane. The d_{31}/d_{33} ratio was derived, taking into account the elastic compliance constants of bulk ceramics. The obtained values between -0.4 and -0.5 are in agreement with bulk ceramic data.

PZT thin films exhibit higher coercive fields (typically 50 kV/cm) and higher break-down voltages (300 kV/cm) than bulk ceramic PZT. It is therefore possible to drive thin film devices with higher fields in order to compensate partially for the smaller thickness (t_p). (The relevant force per unit width of the film is $e_{31,eff} \cdot E_3 \cdot t_p$).

Ultrasonic actuators, such as stators for micromotors or fork structures for resonant sensors, utilize diaphragms or other structures in resonance. Here it is important to consider the influence of the geometry on the coupling constant, and to minimize the stress of the involved films. If the thickness h of the passive part (low stress nitride, silicon) is increased beyond about three times the thickness of the PZT film, the square of the coupling

constant k, k^2, is decreased as h^{-1}, i.e., a smaller fraction of electrical energy can be converted into mechanical work. When k^2 becomes less than tanδ, more energy is dissipated than transformed into mechanical work. The figure of merit of efficiency can be given as: $(e_{31,eff})^2 \cdot t_p/(\varepsilon \cdot \tan\delta)$. Ideally the PZT film thickness is about half as thick as the supporting silicon structure. In this case, an effective coupling constant k_{eff} of 0.40 has been calculated for a cantilever /22/. Tensile film stresses have to be avoided, because they drastically reduce the coupling factor in the range of small silicon thicknesses, where the coupling constant would be highest.

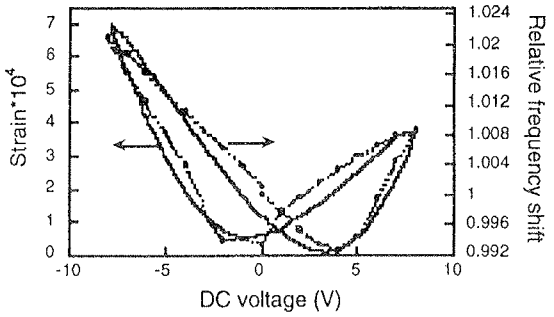

Fig. 4: Normalized strain measured perpendicular to the film plane by optical interferometry, and the normalized frequency shift of a resonating membrane, as a function of the applied dc voltage. The latter is proportional to the in plane stress (from ref. /19/, 0.6μm sputtered PZT 45/55, two different substrates). The piezoelectric coefficients evaluated from the slopes are: $d_{33,eff} = 50$ pm/V, $e_{31,eff} = 4$ C/m².

4.2 Ultrasonic micromotor

The first characterization of a functional PZT thin film micro motor has recently been performed /23,24/. A hybrid type motor was applied, which utilizes static deflection waves of an ultrasonic thin film stator. These are transformed into a rotational movement by an elastic fin rotor /25/. The motor could be operated with voltages of less than 1.0 V_{rms}. A maximal torque of 0.3 μNm was achieved with 2.4 mN normal force applied between stator and rotor. The highest speed observed was 20 rps. Fig. 5 shows a schematic cross section of the motor set-up, and in fig. 6 a picture of the electrode structure is displayed. Moving rotor and gear are shown in the video picture of fig. 7.

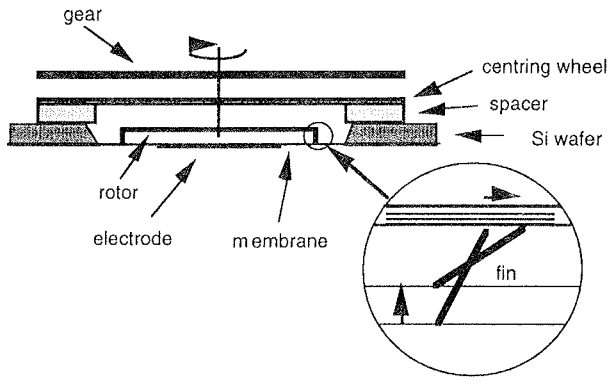

Fig. 5: Schematic cross section through the set-up of the elastic fin motor.

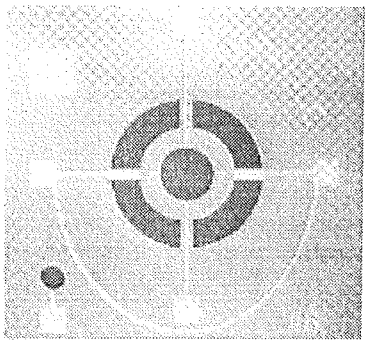

Fig. 6: Image of the ultrasonic stator as seen from the electrode side. The outer diameter of the ring shaped electrode is 3.6 mm (from ref. /24/.

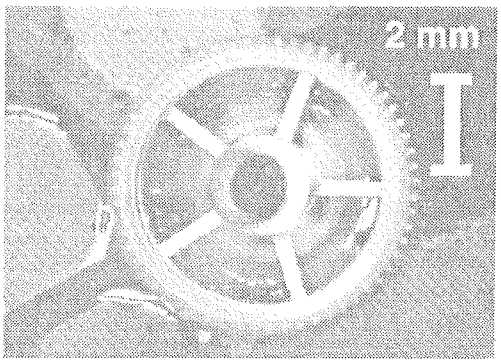

Fig. 7: Video picture of working micromotor. Rotating rotor (bottom) and load wheel (top) are seen. The static wheel fixes the axle (from ref. /23/).

Stators with 1 μm thick sol-gel deposited PZT 45/55 of (111) orientation have been investigated for various thicknesses (15 to 100 μm) of the passive silicon part. In fig. 8 the speed vs. applied ac voltage is displayed. The application of an additional dc bias increases polarization and piezoelectric constant, and thus the rotation speed of the motor. There is a threshold voltage of 0.5 to 1.0 V_{rms} below which there is not enough amplitude for initiating the rotation. Above the threshold, the speed increases linearly with the applied ac voltage, and thus the deflection amplitude. The torque at zero speed saturates at low voltages of 1 to 2 V_{rms} at 0.25 to 0.3 μNm, which must be the value of the frictional torque /25/ for the applied normal force. Speed and torque per voltage, as well as the threshold voltage, did not change with varying silicon thickness. It must be concluded that the motor receives a constant fraction of the mechanical power delivered by the stator, as this power does neither change in the given thickness range.

The output power of the motor was measured as 1 to 2 $\mu W/V_{rms}$ typically (independent of silicon thickness). This is for the thinnest membrane (i.e. 15 μm thick silicon) 4×10^{-4} times the reactive power delivered to the capacitance, and hence also smaller than the dielectric loss power ($\tan\delta = 0.03$). The square of the effective coupling constant k^2_{eff}, measured as 0.03 from impedance measurements, is a rough measure for the amount of electrical energy that is converted into mechanical work of the membrane. The transmission efficiency between stator and rotor therefore seems to be rather small. For an improvement, the normal force needs to be increased, in order to increase the frictional torque.

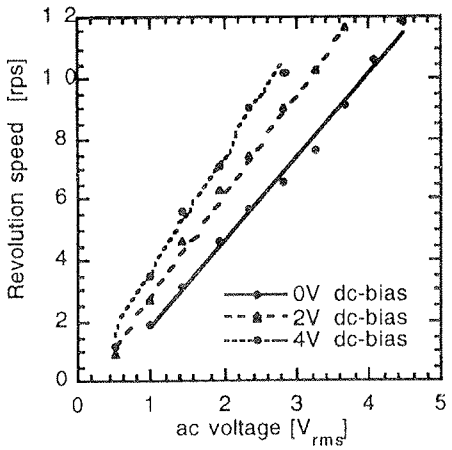

Fig.8: Revolution speed as a function of applied ac voltage for a stator with 50 μm thick silicon and a 1 μm thick PZT film (B_{10} mode at 108.1 kHz, /24/).

5. INFRA-RED DETECTORS

Pyroelectric infra-red detection is a potentially important application for ferroelectric thin films. Compared to bulk devices, thin film devices exhibit a small thermal time constant (t_{th}) and thus work better at higher frequencies, which is interesting for thermal imaging. Several industrial laboratories therefore have programs for the development of 2-dimensional arrays /26/. Due to the small heat capacity of thin film elements, heat conduction to the substrate (acting as heat sink) must be reduced. Silicon micromachining is a very convenient technique to tailor the thermal properties. Very thin ceramic membranes of 0.9 μm can be fabricated in this way as a supporting structure /27/. The thermal insulation by such membranes is so effective that the cooling by air convection becomes dominant /28/.

The output of a pyroelectric can either be measured as a voltage response R_V or a current response R_I. The frequency behavior of a simplified situation is shown in fig. 9. In contrast to bulk sensors, thin film sensors have electrical time constants (t_e typically 10 to 100 s) that are larger than the thermal ones (t_{th} typically 30 ms or smaller). This has an important advantage: The noise voltage drops already in the intermediate frequency range between inverse electrical ($1/t_e$) and inverse thermal time constant ($1/t_{th}$), which is the ideal range for voltage detection (see fig. 10).

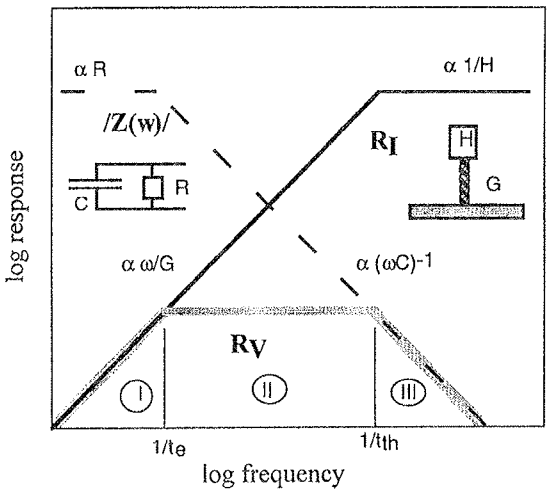

Fig. 9: Log-log scheme of current and voltage response, together with the impedance for the typical thin film situation where the thermal time constant is much shorter than the electrical one. Thermal wave length effects are neglected. (G is the thermal conductivity, H the heat capacity.)

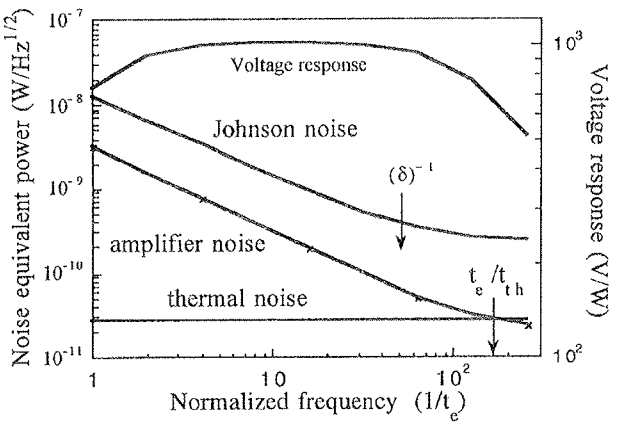

Fig. 10: Noise equivalent powers (NEP) of different sources for a model element with 1 mm^2 surface and cooling by air convection only, calculated from experimentally verified parameters. (Formulas from ref. /31/.) The displayed frequency is normalized to $1/t_e$

An array of 900 x 400 x 1.5 μm elements on Si_3N_4/SiO_2 membranes has been realized /28,29,30/. In order to avoid the above mentioned orientation problem of tetragonal PZT, the 1.6 μm thick PZT 15/85 film was grown in (111) orientation by sol-gel techniques, applying the TiO_2 seed layer. Black platinum was taken as absorbing layer on top of PZT (see fig. 11). A voltage response of 800 V/W was obtained at 1 Hz, and a current

response of 15 μA/W was measured at more than 20 Hz /29,30/ (see fig. 12). Thermal wave length effects account for the increase of the current response above the calculated behavior in fig. 12. The elements exhibited typically a noise voltage of 1 μV at 1 Hz /28/, corresponding to a noise equivalent power of 1.2 nW. This low noise level is in agreement with the calculations of fig. 10. Although the thin film elements do not have yet the sensitivity of $LiTaO_3$ single crystals at the low frequency of 1 Hz, their signal to noise ratio is as good.

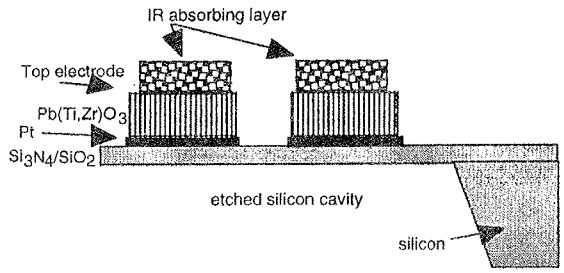

Fig. 11: Typical structure of pyroelectric elements on a thin membrane fabricated by means of micromachining (only a fraction is shown).

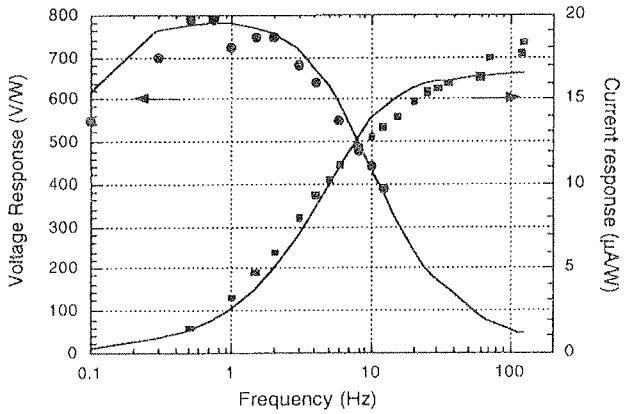

Fig. 12: Measured voltage and current responsivities (dots) as a function of modulation frequency for a PZT pyroelectric array element (from ref. /29/). The full lines are calculated responses.

6. OUTLOOK

Ferroelectric thin films offer alternative solutions for microsystems in the field of microactuators and sensors. Ideal designs still have to be done, especially in the case of piezoelectric devices. Improvement of film properties can certainly be expected, since there is still room for optimizing film composition and microstructure. Thicker films are of great interest, since they allow to increase the force output of actuators, and to decrease the dielectric noise of sensors. Finally, the degradation of PZT films in ac (vibrating structures) and dc applications (switches) has to be studied.

7. ACKNOWLEDGEMENTS

The author wishes to thank his colleagues for many useful discussions. The work has been supported by the Swiss Priority Program on Materials, the Swiss Commission for the Technology and Innovation, and the Program "Microsystems and Microtechnique" of EPFL.

8. REFERENCES

/1/ R.A. Roy, K.F. Etzold, and J.J. Cuomo, "Ferroelectric thin film synthesis, past and present: a selective view", MRS Symp. Proc., vol. 200 ,1990, pp. 141-152.

/2/ R. Bruchhaus, H. Huber, D. Pitzer, and W. Wersing, "Deposition of ferroelectric PZT thin films by planar multi-target sputtering", Ferroelectrics, vol. 127, 1992, pp. 137-142.

/3/ T. Maeder and P. Muralt, "In-situ thin film growth of $PbTiO_3$ by multi target sputtering", MRS Symp. Proc., vol. 341, 1994, pp. 361-366.

/4/ M. Kojima, M.Okuyama, T. Nakagawa and Y. Hamakawa, "Chemical vapor deposition of $PbTiO_3$ films", Jap. J. Appl. Phys., vol. 22, Suppl. 22-2, 1983, pp. 14-17.

/5/ G.J.M. Dormans, P.J. van der Veldhoven and M. de Keijser, "Composition controlled growth of $PbTiO_3$ on $SrTiO_3$ by organometallic chemical vapor deposition", J. Crystal Growth, vol. 123, 1992, pp. 537-544.

/6/ K.D. Budd, S.K. Dey, and D.A. Paine, "Sol-Gel processing of PT, PZ, PZT and PLZT thin films", Brit. Ceram. Proc., vol. 36, 1985, p. 107.

/7/ M. de Keijser, G.J.M. Dormans, "Modelling of organometallic chemical vapor deposition of lead titanate", J. Crystal Growth, vol. 149, 1995, pp. 215-228.

/8/ T. Maeder, P. Muralt, M. Kohli, A. Kholkin, and N. Setter, "$Pb(Zr,Ti)O_3$ Thin Films by In-situ Reactive Sputtering on Micromachined Membranes for Micromechanical Applications", Ceramic Films and Coatings, Sheffield (GB) 1994, British Ceramics Proceedings, vol. 54, 1995, pp. 206-218.

/9/ D.P. Vijay and S.B. Desu, J. Electrochem. Soc., vol. 140, 1993, p. 2640.

/10/ R. Ramesh, H. Gilchrist, T. Sands, V.G. Keramidas, R. Haakenaasen, and D.K. Fork, "Ferroelectric LSCO/PZT/LSCO heterostructres on silicon via template growth", Appl. Phys. Lett., vol. 63, 1993, pp. 3592-94.

/11/ K. Sreenivas, I. Reaney, T. Maeder, N. Setter, C. Jagadish, and R. G. Elliman, "Investigation of Pt/Ti bilayer metallization on silicon for ferroelectric thin film integration", J. Appl. Phys., vol. 75, 1994, pp. 232-239.

/12/ T. Maeder, P. Muralt, L. Sagalovicz, I. Reaney, M. Kohli, A. Kholkin, and N. Setter, "PZT thin films on Zr membranes for micromechanical applications", Appl. Phys. Lett. vol. 68, 1996, pp. 776-778.

/13/ J.S. Speck and W. Pompe, "Domain configurations due to multiple misfit relaxation mechanisms in epitaxial ferroelectric films I", J. Appl. Phys., vol. 76, 1994, pp. 466-476.

/14/ J.S. Speck, A. Seifert, and W. Pompe, "Domain configurations due to multiple misfit relaxation mechanisms in epitaxial ferroelectric films II", J. Appl. Phys., vol. 76, 1994, pp. 477-483.

/15/ A. Seifert, F.F. Lange, and J.S. Speck, "Epitaxial growth of PbTiO3 thin films on (001) SrTiO3 from solution precursors", J. Mater. Res., vol. 10, 1995, pp. 680-691.

/16/ R. Takayama and Y. Tomita, "Preparation of epitaxial PZT thin films and their crystallographic, pyroelectric, and ferroelectric properties", J. Appl. Phys., vol. 65, 1989, pp. 1666-1670.

/17/ K.G. Brooks, I.M. Reaney, R. Klissurska, Y. Huang, L. Bursill, and N. Setter, "Orientation of rapid thermally annealed lead zirconate titanate thin films on (111) Pt substrates", J. Mater. Res., vol. 9, 1994, pp. 2540-2553.

/18/ P. Muralt, T. Maeder, S. Scalese, D. Naumovic, R.G. Agostino, N. Xanthopoulos, H.J. Mathieu, "In-situ sputter deposition of $PbTiO_3$ thin films: nucleation on textured platinum films", Proceedings TATF'96, Colmar, April 1-3, 1996, France, pp. 45-47.

/19/ P. Muralt, A. Kholkin, M. Kohli, and T. Maeder, "Piezoelectric actuation of PZT thin film diaphragms at static and resonant conditions", Sensors and Actuators A, vol. 53, 1996, pp. 397-403.

/20/ A. Kholkin, E. Colla, K. Brooks, P. Muralt, M. Kohli, T. Maeder, D. Taylor, and N. Setter, "Interferometric study of piezoelectric degradation in ferroelectric thin films", Microelectronic Eng., vol. 29, 1995, pp 261-264.

/21/ K. Lefki and G.M. Dormans, "Measurement of piezoelectric coefficients of ferroelectric thin films", J. Appl. Phys., vol. 76, 1994, pp. 1764-1767.

/22/ H. Pavlicek, G. Wachutka, "CAD tools for Mems", UETP MEMS course, Swiss Foundation for Research in Microtechnology, Neuchâtel, Switzerland.

/23/ P. Muralt, M. Kohli, T. Maeder, A. Kholkin, K. Brooks, R. Luthier, and N. Setter, "Fabrication and characterization of PZT thin-film vibrators for micro motors", Sensors and Actuators A, vol. 48, 1995, pp. 157-165.

/24/ M.-A. Dubois, P. Muralt, K.G. Brooks, R. Luthier, "Improved torque of PZT thin film actuated elastic fin micromotor", Proc. Actuator 96, Bremen (Germany) 1996, pp.165-168.

/25/ M. Kurosawa, T. Uchiki, H. Hanada, K. Nakamura, and S. Ueha, "Simulation and experimental study on elastic fin ultrasonic motor", IEEE Ultrasonics Symposium 92, Tucson (USA), 1992 pp. 893-896.

/26/ N.M. Shorrocks, A. Patel, M.J. Walker, A.D. Parsons, "Integrated thin film PZT pyroelectric detector array", Microelectronic Eng., vol. 29, 1995, pp. 59-66.

/27/ A. Bell, Y. Huang, M. Kohli, O. Paul, P. Ryser, and M. Forster, "$PbTiO_3$ thin films for pyroelectric detection", Proc. of Int. Symp. Appl. Ferroelectrics (ISAF'94), Pennsylvania (USA) 1994, pp 691-694.

/28/ M. Kohli, Y. Huang, T. Maeder, C. Wüthrich, A. Bell, P. Muralt, N. Setter, P. Ryser, M. Forster, "Processing and properties of thin film pyroelectric devices", Microelectronic Eng., vol. 29, 1995, pp. 93-96.

/29/ P. Muralt, K. Brooks, M. Kohli, T. Maeder, and Ch. Wüthrich, "Ferroelectric thin films for microsystems", 6th conf. Appl. Surf. Interf. Analysis ECASIA'95, Montreux (Switzerland), 1995, pp. 115-122.

/30/ M. Kohli, C. Wüthrich, K. Brooks, M. Forster, P. Muralt, N. Setter, P. Ryser, "Pyroelectric thin film sensor array", Eurosensors'96, in press.

/31/ R.W. Whatmore, "Pyroelectric devices and materials", Rep. Prog. Phys., vol. 49, 1986, pp. 1335-1386.

Dr. Paul Muralt
EPFL
Departement des Matériaux
Laboratoire de Céramique
MX-D Ecublens
CH-1015 Lausanne, Switzerland
tel.: +41 21 693 49 57
fax: +41 21 693 58 10
E.mail: Paul.Muralt@lc.dmx.epfl.ch

Prispelo (Arrived): 04.09.1996 *Sprejeto (Accepted): 19.11.1996*